

RESEARCH PAPER

Identification and pharmacological characterization of the prostaglandin FP receptor and FP receptor variant complexes

Y Liang¹, DF Woodward¹, VM Guzman¹, C Li¹, DF Scott², JW Wang¹, LA Wheeler¹, ME Garst¹, K Landsverk³, G Sachs², AH-P Krauss⁵, C Cornell⁴, J Martos⁴, S Pettit⁴ and H Fliri⁴

¹Departments of Biological and Chemical Sciences, Allergan Inc., Irvine, CA, USA; ²Department of Membrane Biology, UCLA, Los Angeles, CA, USA; ³Covance Inc., Madison, WI, USA and ⁴Selcia Ltd, Ongar, Essex, England

Background and purpose: A prostamide analogue, bimatoprost, has been shown to be effective in reducing intraocular pressure, but its precise mechanism of action remains unclear. Hence, to elucidate the molecular mechanisms of this effect of bimatoprost, we focused on pharmacologically characterizing prostaglandin FP receptor (FP) and FP receptor variant (altFP) complexes.

Experimental approach: FP receptor mRNA variants were identified by reverse transcription-polymerase chain reaction. The FP-altFP4 heterodimers were established in HEK293/EBNA cells co-expressing FP and altFP4 receptor variants. A fluorometric imaging plate reader was used to study Ca²⁺ mobilization. Upregulation of cysteine-rich angiogenic protein 61 (Cyr61) mRNA was measured by Northern blot analysis, and phosphorylation of myosin light chain (MLC) by western analysis.

Key results: Six splicing variants of FP receptor mRNA were identified in human ocular tissues. Immunoprecipitation confirmed that the FP receptor is dimerized with altFP4 receptors in HEK293/EBNA cells co-expressing FP and altFP4 receptors. In the studies of the kinetic profile for Ca²⁺ mobilization, prostaglandin F_{2α} (PGF_{2α}) elicited a rapid increase in intracellular Ca²⁺ followed by a steady state phase. In contrast, bimatoprost elicited an immediate increase in intracellular Ca²⁺ followed by a second phase. The prostamide antagonist, AGN211335, selectively and dose-dependently inhibited the bimatoprost-initiated second phase of Ca²⁺ mobilization, Cyr61 mRNA upregulation and MLC phosphorylation, but did not block the action of PGF_{2α}.

Conclusion and implications: Bimatoprost lacks effects on the FP receptor but may interact with the FP-altFP receptor heterodimer to induce alterations in second messenger signalling. Hence, FP-altFP complexes may represent the underlying basis of bimatoprost pharmacology.

British Journal of Pharmacology (2008) **154**, 1079–1093; doi:10.1038/bjp.2008.142; published online 21 April 2008

Keywords: prostaglandin; prostamide; intraocular pressure; receptor dimerization; calcium signalling

Abbreviations: altFP, alternative splicing variant of prostaglandin FP receptor; EBNA, Epstein–Barr nuclear antigen; FLIPR, fluorometric imaging plate reader; FP, prostaglandin FP receptor; HEK, human embryonic kidney; MLC, myosin light chain; PGF_{2α}, prostaglandin F_{2α}.

Introduction

Prostaglandin F_{2α} (PGF_{2α}) is a product of cyclooxygenase-catalysed metabolism of arachidonic acid (Smith *et al.*, 1991). It has been identified to be an endogenous ligand of prostaglandin FP receptors. Activation of FP receptors initiated by ligand binding triggers G_sq protein-coupled

mechanisms involving Ca²⁺ signalling, IP₃ turnover and activation of protein kinase C (Toh *et al.*, 1995). PGF_{2α} has diverse physiological actions that include causing smooth muscle contraction (Horton and Poyser, 1976), stimulating DNA synthesis and cell proliferation, and cardiac myocyte hypertrophy (Adams *et al.*, 1996). Importantly, PGF_{2α} analogues have been used clinically to reduce ocular hypertension (Woodward *et al.*, 1993). Although the precise mechanisms involved remain unclear, the effects of PGF_{2α} analogues on intraocular pressure (IOP) principally involve an increase in uveoscleral outflow of aqueous humor. These events involve secretion of metalloproteinases by ciliary

Correspondence: Dr Y Liang, Allergan Inc., 2525 Dupont Dr, Irvine, CA 92612, USA.

E-mail: liang_yanbin@allergan.com

⁵Current address: Pfizer, 10724 Science Center Drive, San Diego, CA, USA
Received 29 December 2007; revised 21 February 2008; accepted 29 February 2008; published online 21 April 2008

smooth muscle cells and remodelling of the extracellular matrix with a resultant widening of intermuscular spaces (Gaton *et al.*, 2001; Weinreb and Lindsey, 2002; Richter *et al.*, 2003).

In contrast to prostaglandin $F_{2\alpha}$, prostamides (prostaglandin ethanalamides) were recently identified as a new class of compounds that was formed from anandamide via metabolic transformation catalysed by cyclooxygenase-2 (Yu *et al.*, 1997; Burstein *et al.*, 2000; Kozak *et al.*, 2001; Koda *et al.*, 2003). Although their physiological actions have not been fully investigated, a synthetic prostamide analogue (bimatoprost) has been shown to be very effective in reducing IOP by increasing both uveoscleral and trabecular outflow of aqueous humor (Woodward *et al.*, 2001). The activities of prostamides as endogenous ligands at prostaglandin receptor(s) have been investigated, but have been shown to exert no meaningful activity (Berglund *et al.*, 1999; Woodward *et al.*, 2001; Ross *et al.*, 2002; Matias *et al.*, 2004). Studies on their metabolic rate clearly demonstrate that prostamides and their synthetic analogue bimatoprost exert their *in vitro* pharmacological effects (Matias *et al.*, 2004) and ocular hypotensive effects as the intact molecule (Woodward *et al.*, 2003). Experimental evidence suggests that prostamides may act as endogenous ligands at their own receptors (prostamide receptors) (Woodward *et al.*, 2001, 2003; Matias *et al.*, 2004). Nevertheless, prostamide activity has not, so far, been demonstrated in the absence of FP receptor activity. However, results from studies on FP-knockout mice have shown that the effects of bimatoprost on IOP are dependent on an intact FP receptor gene (Crowston *et al.*, 2005; Ota *et al.*, 2005); a single application of bimatoprost did not reduce IOP in FP receptor knockout mice, indicating that FP signalling is required for the early IOP response to bimatoprost. This raised the possibility that bimatoprost may interact with FP receptor gene products, such as spliced variants of the FP receptor or FP receptor complexes, such as FP receptor dimerizing or oligomerizing with FP spliced variants or other receptors. It seemed reasonable, therefore, to investigate newly discovered alternative splicing variants of FP receptor mRNA for their potential to interact with bimatoprost.

Methods

Total RNA isolation

Human eyes were obtained from the National Disease Research Interchange (NDRI, Philadelphia, USA). These eyes were hemisected along the ora serata to expose the posterior chamber of the anterior segment. After the lens had been removed by clipping the zonules, the ciliary body was peeled away from the sclera and placed in ice-cold phosphate-buffered saline.

Total RNA was isolated from human ciliary bodies and human embryonic kidney 293/Epstein-Barr nuclear antigen (HEK293/EBNA) cell lines using RNeasy Kit (Qiagen Inc., Valencia, CA, USA), according to the manufacturer's instruction. RNA concentrations were determined by u.v. spectrophotometry (Beckman DU640) at 260 nm, and stored at -80°C .

Reverse transcription-polymerase chain reaction

Using 2 μg of human total RNA, first-strand cDNA was synthesized by SuperScript II Reverse Transcriptase (Invitrogen, Carlsbad, CA, USA). Samples, 20 μL , containing 2 μg of RNA, 100 ng random primers and 50 U reverse transcriptase were incubated at 42°C for 50 min and terminated by 75°C for 15 min.

The PCR buffer contained 40 mM Tricine-KOH (pH 9.2), 15 mM KOAc, 3.5 mM $\text{Mg}(\text{OAc})_2$, 0.2 mM of each dNTP, 0.2 μM upstream primer (p1: 5'-tgcaatgcaatcacaggaatt-3') and downstream primer (p2: 5'-cactccacagcattgactgg-3'), and 1 U Advantage cDNA polymerase in a final volume of 50 μL . After an initial incubation for 5 min at 94°C , samples were subjected to 35 cycles of 30 s at 94°C , 30 s at 58°C and 30 s at 72°C in a PE9700 thermal cycler.

The PCR products were isolated from 1.5% low-melting agarose gel and subcloned into PCR II TOPO vector (Invitrogen). Sequence analysis was performed by Sequetech (Mountain View, CA, USA). Sequence alignments and analysis were done using the National Center for Biotechnology Information database.

Subcloning and plasmid transfection

Full-length FP and alternative splicing variant of prostaglandin FP receptor (altFP) receptor cDNAs were isolated and subcloned into retrovirus vector (Invitrogen). The plasmids were designated QhFP-wt and QhFP-alt. QhFP-wt or QhFP-alt were transfected into GP2-293 packaging cells. After 72 h, the supernatants containing virus were harvested and centrifuged at 800 g for 15 min to remove cell debris. Virus stock was titrated and stored at -80°C . HEK293/EBNA cells were grown in 6-cm dishes containing Dulbecco's modified Eagle's medium with 10% fetal bovine serum. The cells were infected with QhFP-wt or QhFP-alt, or co-infected with both QhFP-wt and QhFP-alt in equal amounts of virus. After 24 h of infection, the virus-containing medium was removed and replaced with fresh medium containing hygromycin for cell clone selection. Hygromycin-resistant colonies were amplified and screened for expression of FP and altFP receptors. The established cell lines were maintained in the same media as the parental lines.

Epitope tagging of FP receptors and altFP receptors

Wild-type FP and altFP receptors were tagged at their amino termini with either two repeats of haemagglutinin (HA) nonapeptide (YPYDVPDYA) separated by a Gly residue or with two repeats of a Flag sequence (DYKDDDDK), also separated by a Gly residue. Because the FP receptors containing two Flag epitopes or HA epitopes at the amino terminus may not localize to the cell membrane (Fujino *et al.*, 2000), we introduced a prolactin signal peptide preceding the Flag sequence to create Pro-Flag-FP and preceding the HA sequence to create Pro-HA-altFP, according to methods previously described (Kolodziej and Young, 1991). Pro-Flag-FP or Pro-HA-altFP cDNA encoded the amino terminus MDSKGSSQKGSRLLLLVVSNLLLCQGVVS/DYKDDDK... or MDSKGSSQKGSRLLLLVVSNLLLCQGVVS/YPYDVPDYA...representing the prolactin signal peptide,

signal peptidase site(/), Flag epitope-FP or HA epitope-altFP. The prolactin signal peptide was then cleaved by signal peptidase after expression. All of the tagged FP or altFP receptors were subcloned into lentivirus expression vector to create Lenti-Pro-Flag-FP and Lenti-Pro-HA-altFP expression plasmids. All of the plasmids were transfected into 293FT packaging cell lines. After 48 h transfection, the virus containing cell medium was collected, titered and stored at -80°C . HEK293/EBNA cells were grown in 6-cm dishes containing Dulbecco's modified Eagle's medium with 10% fetal bovine serum. The cells were infected with an equal amount of virus. After 24 h of infection, the virus-containing medium was removed and replaced with fresh medium containing blasticidin for cell clone selection. Blasticidin-resistant colonies were amplified and screened for expression of Flag-FP and HA-altFP receptors. The established cell lines were maintained in the same medium as the parental lines.

Northern blot analysis

Total RNA (10 μg) was denatured at 65°C in RNA loading buffer (Ambion Inc., Austin, TX, USA) for 15 min and separated on 1.2% agarose gels containing 0.66 M formaldehyde. RNA loading was assessed by ethidium bromide staining of 28S and 18S ribosomal RNA bands. The relative intensities of 28S and 18S ribosomal RNA bands were used as internal controls to normalize the hybridizations. Human 1.4-kb *Cyr61* (+60 to +1459; GenBank accession no. AF003594) gene-specific DNA fragment was radiolabelled using an $[\alpha\text{-}^{32}\text{P}]\text{-dCTP}$ and Klenow (Ambion Inc.). The blots were hybridized with the gene-specific probes in 50% formamide, $4 \times \text{SSC}$, $1 \times \text{Denhardt's}$ solution, 50 mM sodium phosphate (pH 7.0), 1% sodium dodecyl sulphate (SDS), 50 $\mu\text{g mL}^{-1}$ yeast tRNA and 0.5 mg mL^{-1} sodium pyrophosphate at 42°C overnight and washed with SSC and 0.1% SDS twice at 42°C and with $0.1 \times \text{SSC}$ and 0.1% SDS twice at 42°C . The hybridized blots were exposed to phosphor screens, and the exposed screens were analysed in a PhosphorImager (Amersham Biosciences, Pittsburgh, PA, USA).

Immunoprecipitation and western blotting

HEK293/EBNA cells were cultured in six-well plates. The confluent cells were harvested, washed and lysed in ice-cold lysis buffer containing 150 mM NaCl, 50 mM Tris HCl (pH 8.0), 1 mM EDTA, 1% Triton X-100, 10 mM NaF, 10 mM sodium pyrophosphate, 100 mM sodium orthovanadate plus protease inhibitor mixture. The cell lysates were centrifuged at 14 000 g , at 4°C , for 10 min. For immunoprecipitation, the supernatant fractions were collected and then incubated at 4°C with HA11 (HA antibody) for 15 h. The incubation was continued for another 1 h in the presence of 50 μL of a 1:1 slurry of protein G agarose (Pierce, Rockford, IL, USA) at 4°C . The beads were washed three times with lysis buffer, Laemmli sample buffer was added and the samples were boiled for 5 min and centrifuged at 12 000 g for 10 min. The supernatant fractions were subjected to western blot. In general, the supernatant fraction from immunoprecipitation or from cell lysates of transfected HEK293/EBNA cells were

collected and electrophoresed on 10% SDS-polyacrylamide (SDS-PAGE) gels. Proteins were transferred to polyvinylidene fluoride membrane, and the blots were incubated with a 1:1000 dilution of a monoclonal HA11 or anti-Flag M2 antibody for 1 h at room temperature with rotation. The blots were washed three times and incubated for 1 h at room temperature with a 1:5000 dilution of a goat anti-mouse secondary antibody (Bio-Rad, Hercules, CA, USA) conjugated with horseradish peroxidase. After being washed three times, immunoreactivity of the samples was detected using an immune-star HRP developer system (Bio-Rad).

MLC phosphorylation

HEK293/EBNA cells were cultured in 10-cm plates. The cells were deprived of nutrients in Opti-MEM for 24 h before being pretreated with 2-[3-(5-fluoro-2-propylcarbamoyl-methoxybenzyl)-7-oxabicyclo[2.2.1]hept-2-ylloxazole-4-carboxylic acid (4-cyclohexylbutyl) amide (AGN211335) for 15 min, followed by treatment with $\text{PGF}_{2\alpha}$ or bimatoprost for 30 min. The cell lysates were boiled for 5 min and centrifuged at 12 000 g for 10 min. The supernatant fractions were collected and electrophoresed on 10% SDS-PAGE gels. Proteins were transferred to polyvinylidene fluoride membrane, and the blots were incubated with a 1:1000 dilution of a phosphorylated myosin light chain (MLC) antibody or MLC antibody for 16 h at 4°C with rotation. The blots were washed three times and incubated for 1 h at room temperature with a 1:3000 dilution of a goat anti-rabbit secondary antibody (Bio-Rad) conjugated with horseradish peroxidase. After being washed three times, immunoreactivity of the samples was detected using an immune-star HRP developer system (Bio-Rad).

Calcium signal studies using a FLIPR instrument

HEK293/EBNA cells were seeded at a density of 50 000 cells per well in Biocoat poly-D-lysine-coated black-well, clear-bottom 96-well plates (Becton-Dickinson) and allowed to attach overnight. Before the assay, the cells were washed twice with Hank's balanced salt solution-HEPES buffer (without bicarbonate and phenol red, 20 mM HEPES, pH 7.4) using a Lab Systems Cellwash plate washer. After being subjected to 45 min of dye loading (fluo-4 AM, 2 μM) in the dark at 37°C in 5% CO_2 humidified atmosphere, the plates were washed three times with Hank's balanced salt solution-HEPES buffer to remove excess dye leaving 100 μL buffer in each well. Plates were equilibrated to 37°C for 3 min prior to processing within the fluorometric imaging plate reader (FLIPR). The peak increase in fluorescence counts was recorded for each well. All data points were determined in triplicate. Mock-transfected cells (transfected with empty plasmid) were screened in parallel with FP- and alternative FP-co-transfected cells.

Prostamide antagonist

pA₂ determination. The methods used to study the effects of antagonists of prostamide $\text{F}_{2\alpha}$ on bimatoprost-induced feline iridial stimulation and associated data analysis were identical

to those previously described in more detail (Wan *et al.*, 2007; Woodward *et al.*, 2007). Briefly, feline iridial tissue specimens were mounted vertically under 50–100 mg tension in 10 mL jacketed organ baths. These contained Krebs solution maintained at 37 °C and gassed with 95% O₂ and 5% CO₂. Measurement of contractile activity was by means of force displacement transducers and was recorded on a polygraph chart recorder. After a 1-h equilibration period, vehicle and antagonist (AGN211335) were administered 30 min before the agonist dose–response curve was constructed. Agonist concentration–response curves were compared in the presence and absence of graded doses of antagonist (AGN211335). PGF_{2α} (10^{−7} M) was used at the beginning and end of each dose–response experiment as a reference compound. The pA₂ value for AGN211335 was obtained by plotting log₁₀ concentration–response-1 vs log₁₀ [antagonist] according to the method of Arunlakshana and Schild (1959), using Graphpad Prism 4 software (Woodward *et al.*, 2007). Feline iridial experiments were performed by Covance Inc. (Madison, WI, USA).

Human recombinant prostaglandin receptors. Studies on human recombinant prostaglandin receptors were as previously described (Woodward *et al.*, 2003; Matias *et al.*, 2004). These involved Ca²⁺ signal studies and the use of a FLIPR instrument. The use of chimeric G protein cDNAs allowed responses to Gs- and Gi-coupled receptors to be measured as a Ca²⁺ signal. Thus, prostaglandin DP, EP₂ and EP₄ receptor cDNAs were co-transfected with chimeric Gqs cDNA, and EP₃ receptor cDNA was co-transfected with chimeric Gqi cDNA (Molecular Devices, Sunnyvale, CA, USA), each containing a haemagglutinin (HA) epitope to detect protein expression.

Stable transfection in HEK293/EBNA cells was achieved using the same vectors and Fugene 6 method as previously described. Stable transfectants were selected according to hygromycin resistance. FLIPR studies were performed as described in the previous section. AGN211335, 3 × 10^{−5} M, was given as a 10 min pretreatment, vehicle control wells were pretreated with an equal volume of ethanol. Agonists used for each receptor are listed as follows: BW245C for DP; PGE₂ for EP_{1–4}; PGF_{2α} for FP; carbaprostacyclin for IP and U-46619 for IP receptors. The peak fluorescence change in each well containing the drug was expressed relative to the controls. No activity was observed at DP_{1–2}, EP_{1–4}, FP or IP receptors for 3 × 10^{−5} M AGN211335. AGN211335 was a TP antagonist with a k_b of 101 nM.

Activity at DP₂ (CRTH2) receptors was determined by externally using a proprietary FLIPR-based assay (GPCRProfiler, Millipore Corp., St Charles, MO, USA). The experimental conditions were identical to those employed at Allergan Inc.; PGD₂ was used as an agonist in this assay. AGN211335, 3 × 10^{−5} M, was found to have no activity at the DP₂ receptor.

Drugs

AGN211335 was synthesized by Selcia Ltd (Ongar, Essex, UK). Bimatoprost and PGF_{2α} were purchased from Cayman Chemical Co. (Ann Arbor, MI, USA). All stock solutions were prepared in ethanol. Screening methods for the prostamide antagonist, AGN211335, were as previously described (Woodward *et al.*, 2007).

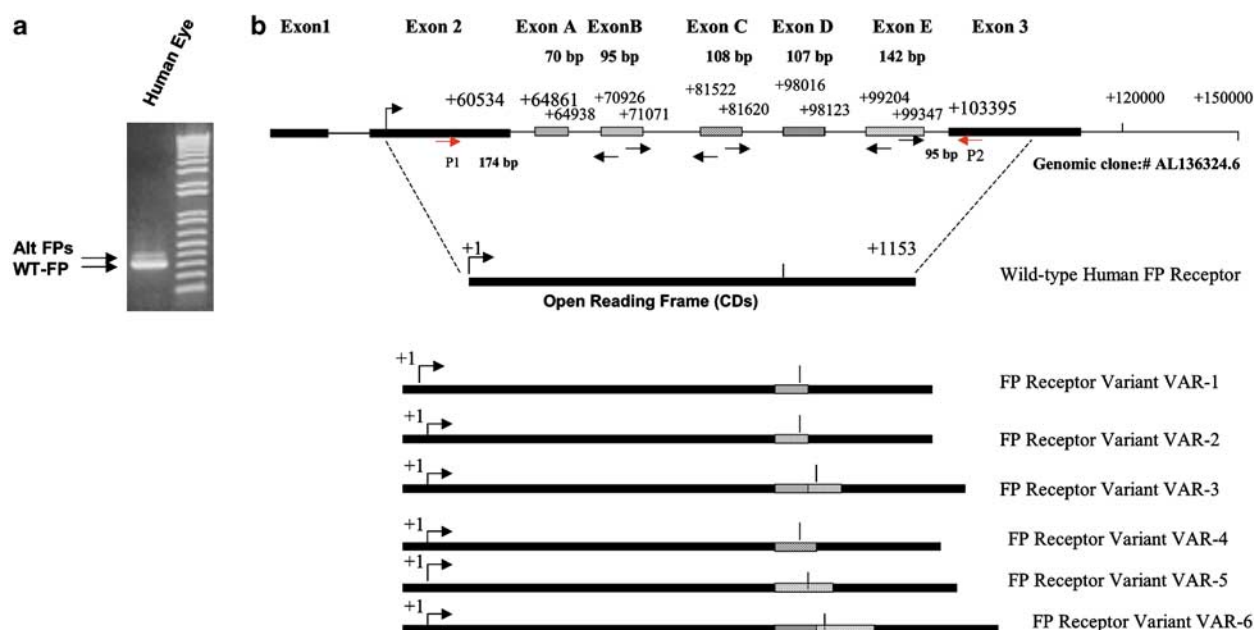


Figure 1 Reverse transcription-polymerase chain reaction analysis of the FP receptor gene in human ciliary bodies. (a) The location of PCR products of the correct size for known wild-type FP receptor, abbreviated as WT-FP, and FP receptor variants, abbreviated as altFP, are indicated by arrows. Sequencing analysis showed that the band of altFP contains multiple FP receptor variants. (b) The black bars represent the coding sequence for the wild-type FP receptor. There are five additional exons generated by mRNA alternative splicing, located between exon 2 and exon 3 and indicated as exon A, exon B, exon C, exon D and exon E.

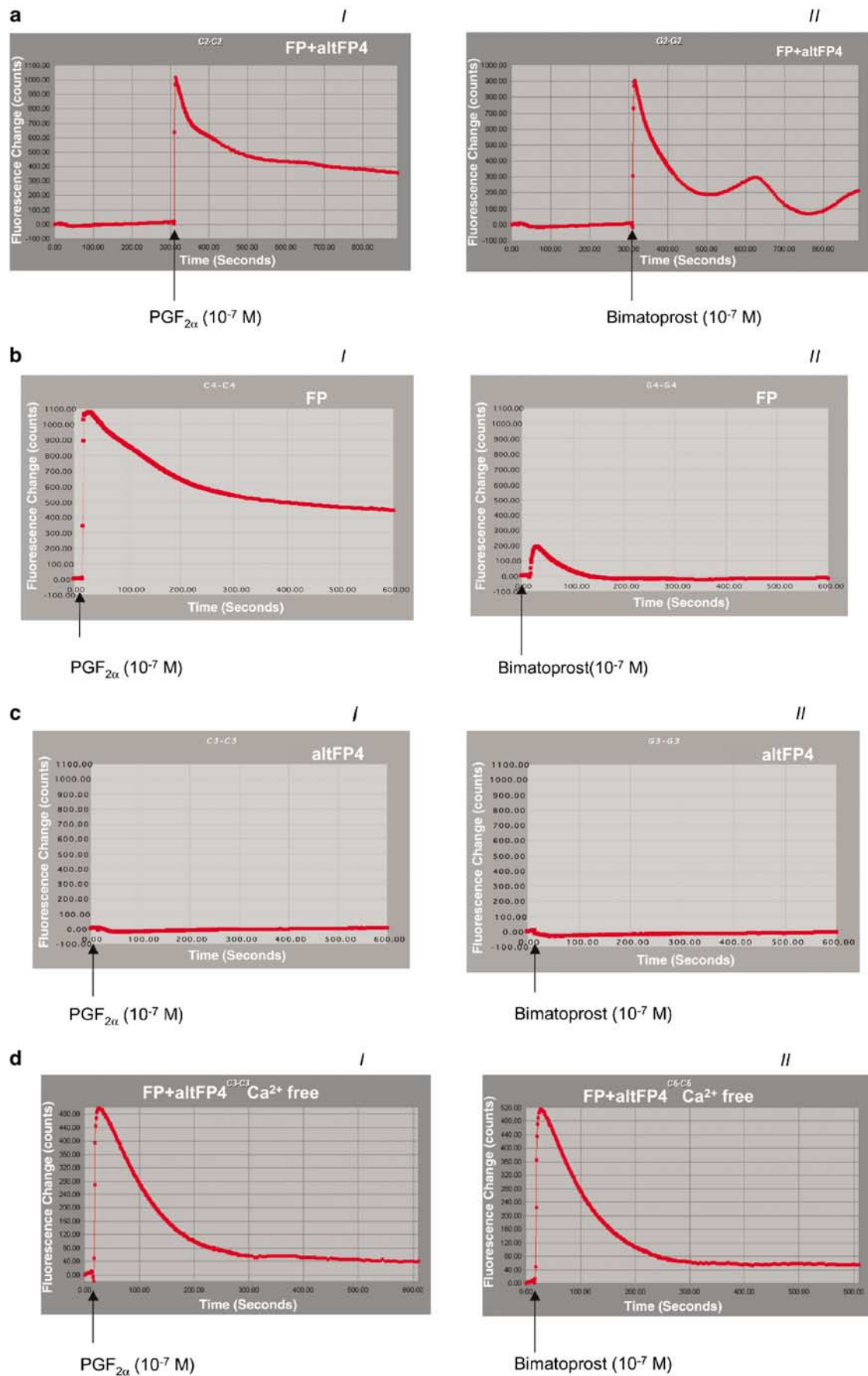


Figure 4 Continued.

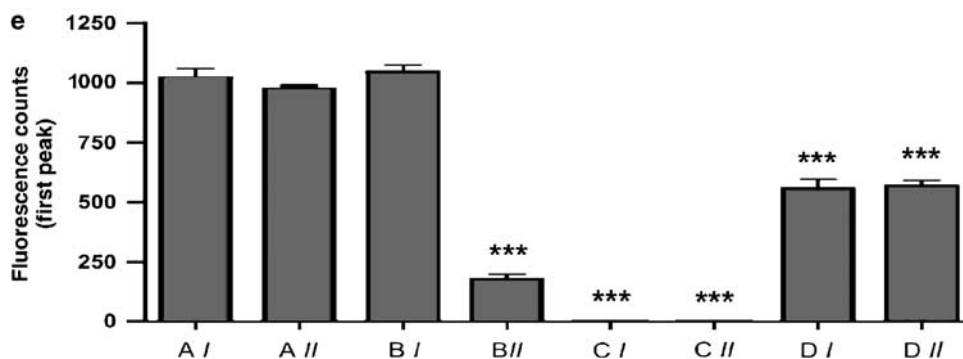


Figure 4 Ca^{2+} signalling of HEK293/EBNA cells co-expressing FP and altFP4 receptors following prostaglandin $\text{F}_{2\alpha}$ ($\text{PGF}_{2\alpha}$) and bimatoprost treatments. (a) Real-time fluorescence traces were recorded by fluorometric imaging plate reader (FLIPR) in HEK293/EBNA cells co-expressing FP and altFP4 receptors following $\text{PGF}_{2\alpha}$ (10^{-7} M) or bimatoprost (10^{-7} M) treatment. (I) After recording baseline for 300 s, 10^{-7} M $\text{PGF}_{2\alpha}$ was added and recorded for additional 600 s. (II) After recording baseline for 300 s, 10^{-7} M bimatoprost was added and recorded for additional 600 s. (b) Real-time fluorescence traces were recorded by FLIPR following $\text{PGF}_{2\alpha}$ (10^{-7} M, I) or bimatoprost (10^{-7} M, II) in HEK293/EBNA cells expressing wt-FP receptor. Real-time fluorescence traces were recorded immediately following $\text{PGF}_{2\alpha}$ (10^{-7} M) or bimatoprost (10^{-7} M) treatment. (c) Real-time fluorescence traces were recorded by FLIPR in HEK293/EBNA cells expressing altFP4 receptor following $\text{PGF}_{2\alpha}$ (10^{-7} M, I) or bimatoprost (10^{-7} M, II) treatment for 600 s. (d) Real-time fluorescence traces were recorded by FLIPR in HEK293/EBNA cells co-expressing FP and altFP4 receptors following $\text{PGF}_{2\alpha}$ (10^{-7} M, I) or bimatoprost (10^{-7} M, II) treatment in Ca^{2+} -free buffer for 600 s. (e) The first peak increase of fluorescence counts was recorded in each treatment (aI–dII). The data represent mean \pm s.d. of three independent experiments. *** $P < 0.01$ versus $\text{PGF}_{2\alpha}$ treatment (aI).

Statistical analysis

Data are expressed as mean \pm s.d. A significant difference between treatments was assessed by the one-way ANOVA, followed by a Bonferroni's *post* test procedure for multiple comparisons. Differences between treatments were considered to be significant if $P < 0.05$. All statistical values were calculated using Graphpad Prism 4 software (GraphPad, San Diego, CA, USA).

Results

Identification of prostaglandin FP receptor variants in human eyes

To identify potential alternative mRNA splicing variants of the human FP receptor, reverse transcription-polymerase chain reaction analyses were performed using human ciliary body cDNA libraries and two FP-specific primers, p1, which is complementary to FP exon 2 sequence, and p2, which is complementary to FP exon 3 sequence. PCR products were subcloned and sequenced (Figure 1a). Sequence analysis showed that there are five additional exons between exon 2 and exon 3 (Figure 1b). The human FP receptor gene contains three exons. The coding region of the FP receptor is located within exon 2 and exon 3. An insertion of the additional exon in the coding region causes frame shifts that lead to encode C terminus-truncated FP receptors (altFPs). Figure 2 shows the deduced amino-acid sequences of human FP (FP) and FP variants (altFPs). The FP and altFPs are identical up to amino acid 266 (leucine-266), at which point there is an insertion of additional exon A, exon B, exon C and exon E to form altFP1, altFP2, altFP4 and altFP5, respectively, and an insertion of two additional exons, exon A and B to form altFP3 and two additional exons, exon D and exon E to form altFP6. The amino-acid sequences of altFPs diverge from those of FP at leucine 266, which is close to the predicted carboxyl terminal end of TM6. For the human

wild-type FP receptor, there are a total of 93 amino acids downstream of leucine-266, which constitute the third extracellular loop (–19 amino acids), TM7 (–22 amino acids) and the intracellular carboxyl terminus (–52 amino acids). A hydrophobic profile analysis of FP and altFPs shows that all altFPs do not have a seventh TM domain and that its carboxyl terminus is extracellular. All altFPs were stably expressed in HEK293/EBNA cell lines. Cells expressing alternative FP receptor mRNA splicing variants were screened with FP ligands and bimatoprost using the FLIPR assay and could not be activated by $10 \mu\text{M}$ $\text{PGF}_{2\alpha}$ or bimatoprost (data not shown). This is entirely consistent with data from a previous study demonstrating that the first alternative variant of human FP receptor RNA (Vielhauer *et al.*, 2004) is not the prostamide receptor. We thought that altFPs, as six-domain receptors, form dimers with FP receptors and function as regulators of the FP receptor. The next experiments were done to determine whether altFPs could form dimers with FP and to characterize their functions. Initial screening of the HEK293/EBNA cells co-transfected FP with each of altFPs (altFP1 and altFP6) showed that the co-transfected HEK293/EBNA cells responded to bimatoprost with a similar Ca^{2+} mobilization profile to that of Ca^{2+} mobilization. As the longer C terminus of altFP4 provides a better prognosis for, perhaps, eventually designing a specific antibody to this isoform, we focused on characterizing the pharmacology of FP and its interaction with the altFP4 receptor heterodimer in the following studies.

Physical interactions between FP and altFP4 receptors

We initially developed stable cell lines of HEK293/EBNA cells expressing epitope-tagged FP and altFP receptors because this cell type has a high transfection efficiency and wide application in studies involving G protein-coupled receptors. Infection of HEK293/EBNA cells with Lenti-Pro-HA-altFP4 or

with Lenti-Pro-Flag-FP or co-infection of HEK293/EBNA cells with Lenti-Pro-HA-altFP4 and Lenti-Pro-Flag-FP, with an equal amount of virus, resulted in the appearance of multiple

bands on immunoblots that were immunoreactive to HA11, a mouse monoclonal anti-HA antibody (Figure 3a, lanes 2 and 3). These bands were not present in the control cells

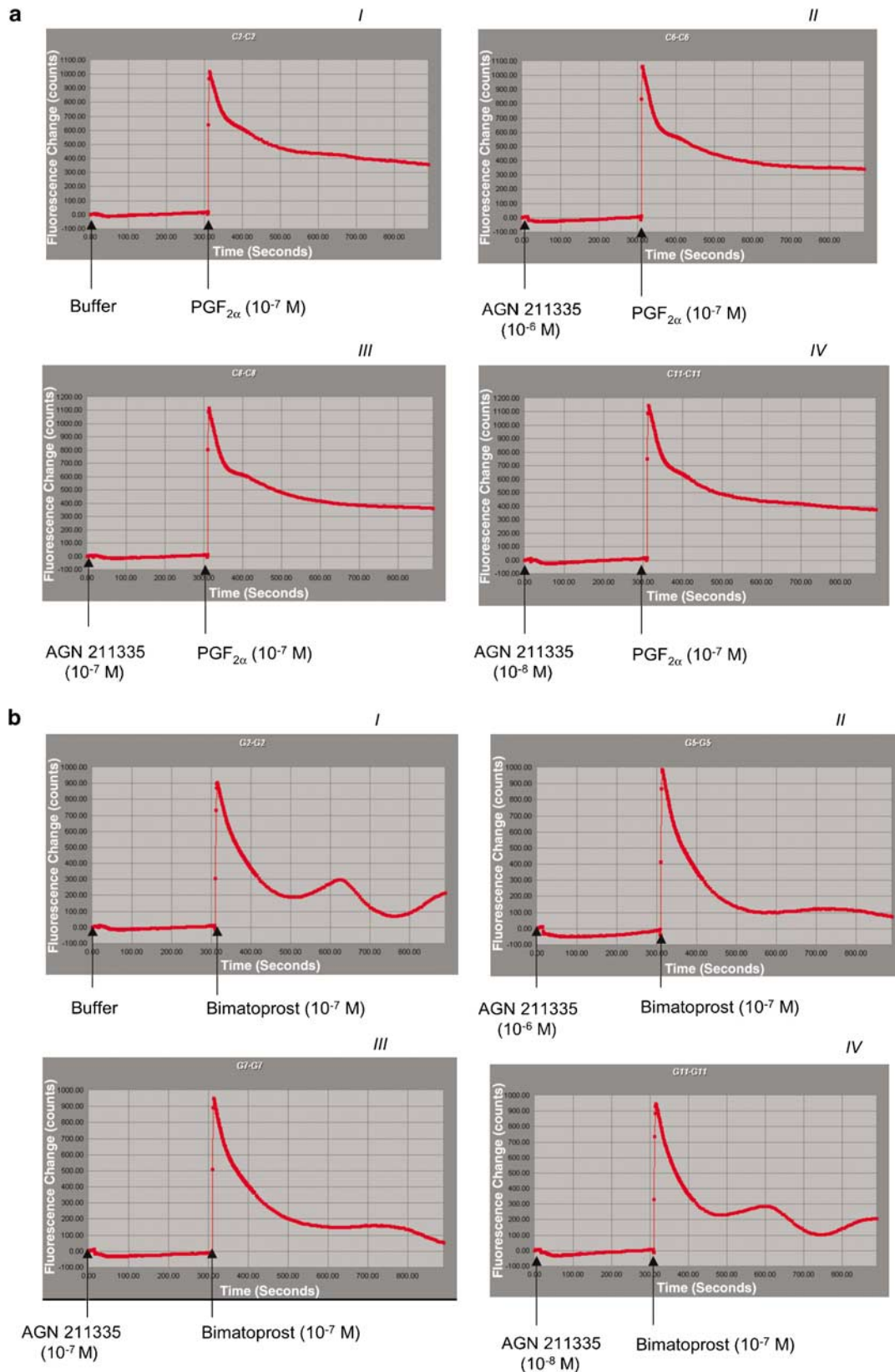


Figure 5 Continued.

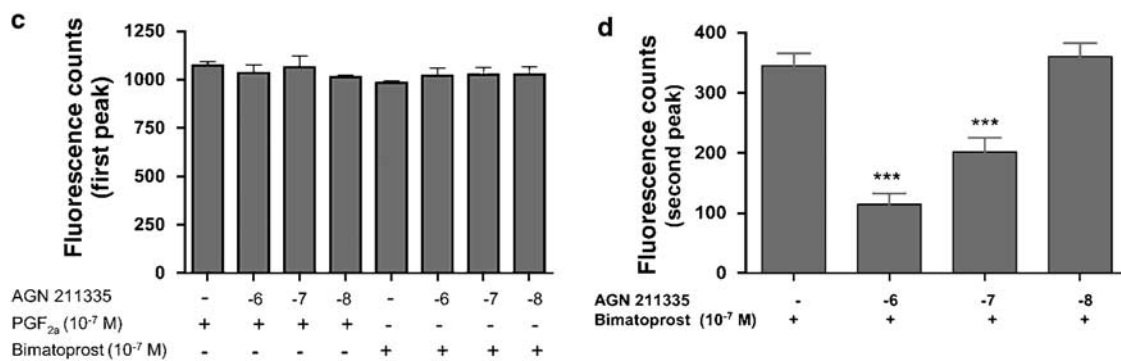


Figure 5 The prostamide-selective antagonist, AGN211335, inhibited bimatoprost-initiated second-phase Ca^{2+} mobilization in HEK293/EBNA cells co-expressing FP and altFP4 receptors. Real-time fluorescence traces were recorded by fluorometric imaging plate reader instrumentation in HEK293/EBNA cells co-expressing FP and altFP4 receptors following the antagonist protocol. (a) HEK293/EBNA cells co-expressing FP and altFP4 receptor pretreated with buffer (I), AGN211335 at 10^{-6} M (II), AGN211335 at 10^{-7} M (III) and AGN211335 at 10^{-8} M (IV) for 300 s, immediately followed by 10^{-7} M prostaglandin $\text{F}_{2\alpha}$ ($\text{PGF}_{2\alpha}$) treatment for 600 s. (b) HEK293/EBNA cells co-expressing FP and altFP4 receptors pretreated with buffer (I), AGN211335 at 10^{-6} M (II), AGN211335 at 10^{-7} M (III) and AGN211335 at 10^{-8} M (IV) for 300 s, immediately followed by 10^{-7} M bimatoprost treatment for 600 s. (c) The first peak increase of fluorescence counts was recorded for each treatment (aI–aIV). The data represent mean \pm s.d. of three independent experiments. No significant differences between treatments were observed. (d) The second peak increase of fluorescence counts was recorded after bimatoprost treatment (bI–bIV). The data represent mean \pm s.d. of three independent experiments. *** $P < 0.01$ versus bimatoprost alone (bI).

(Figure 3a, lane 1), indicating that they represent altFP4 and FP receptor proteins. Figure 3a shows that the molecular weights of the bottom bands in both lane 2 and lane 3 were 33 kDa, which is very close to the calculated molecular mass of epitope-tagged altFP4 receptor, 34 kDa. Higher molecular weight top bands were also observed, a 66 kDa in lane 2, which is close to the calculated molecular weight mass of altFP4 homodimer, 68 kDa, and a 75 kDa in lane 3, which is very close to the calculated molecular weight mass of FP-altFP4 heterodimer, 74 kDa, suggesting that altFP4 receptors form homodimers (Figure 3a, lane 2) and that FP and altFP4 co-transfection (Figure 3a, lane 3) also formed heterodimers (FP molecular weight is higher than the altFP4 receptor).

To clarify whether the higher molecular weight band (75 kDa; Figure 3a, lane 3) was derived from receptor heterodimerization or association with other unknown proteins, we conducted differential immunoprecipitation in which two different epitope-tagged receptors, HA-altFP4 and Flag-FP, were co-expressed and subjected to immunoprecipitation with anti-HA antibody, HA11, against HA-tag and then resolved on SDS-PAGE and immunoblotted with anti-Flag M2 an antibody against the Flag-tag FP receptor. As shown in Figure 3b (lane 3) when Flag-FP and HA-altFP4 receptors were co-expressed in HEK293/EBNA cells, Flag-FP receptors were clearly present in HA antibody-derived immunoprecipitates (Figure 3b, lane 3), which further confirms that the 75-kDa band (Figure 3a, lane 3) is an FP-altFP4 heterodimer. When HEK293/EBNA cells were separately transfected with Flag-FP or HA-altFP4 receptors, no Flag-tagged receptor (Flag-FP) was immunoprecipitated with HA antibody (Figure 3b, lane 1), and no HA-tagged receptor (HA-altFP4) was immunoblotted with Flag antibody (Figure 3b, lane 2). Again, the Flag-tag FP receptor was seen only in the co-transfected HEK293/EBNA cells (Figure 3b, lane 3).

Functional studies of FP receptor and altFP4 receptor dimerization. To investigate the effects of $\text{PGF}_{2\alpha}$ and bimatoprost on

FP-altFP4 receptor heterodimer, we performed Ca^{2+} mobilization studies on HEK293/EBNA cells co-expressing epitope-tagged HA-altFP4 and Flag-FP and HEK293/EBNA cells co-expressing FP and altFP4 receptors, using a FLIPR. Both HEK293/EBNA cell lines showed exactly the same kinetic profile for Ca^{2+} mobilization induced by $\text{PGF}_{2\alpha}$ or bimatoprost, indicating that epitopes contained in the amino terminus of the FP and altFP4 receptors did not disrupt the expression or functions of these receptors. In this study, we used HEK293/EBNA cell lines co-expressing FP and altFP4, expressing only FP and only altFP4 as cell models. Figure 4 shows that $\text{PGF}_{2\alpha}$, 10^{-7} M, activated FP-altFP4 (Figure 4aI) and the FP receptor (Figure 4bI). There was no difference between only FP and FP-altFP4 in response to $\text{PGF}_{2\alpha}$ in terms of first peak of fluorescence counts and kinetic profiles. Both $\text{PGF}_{2\alpha}$ and bimatoprost at 10^{-7} M activated the FP-altFP4 receptor heterodimer; the first peak of fluorescence counts for bimatoprost treatment were very close to those of $\text{PGF}_{2\alpha}$ (Figure 4aI and II). The kinetic profiles of real-time fluorescence traces for $\text{PGF}_{2\alpha}$ and bimatoprost treatments were different. $\text{PGF}_{2\alpha}$ elicited a robust and rapid increase in intracellular Ca^{2+} concentration followed by a steady-state phase within the time course of the experiment (600 s, count from the initiation of a rapid Ca^{2+} increase) (Figure 4aI). In contrast, bimatoprost elicited an immediate and robust increase in intracellular Ca^{2+} concentration followed by a second phase Ca^{2+} wave within the time course of the experiment (600 s) (Figure 4aII). This observation accords well with the results obtained in Ca^{2+} signalling studies in cat iris sphincter cells stimulated by bimatoprost. Bimatoprost was shown to elicit an immediate increase in intracellular Ca^{2+} concentration followed by a second Ca^{2+} wave, suggesting the existence of a native FP-altFP4 receptor heterodimer in cat iris sphincter cells (Spada *et al.*, 2005). Although $\text{PGF}_{2\alpha}$ markedly stimulated the wild-type FP receptor, bimatoprost produced not more than a residual effect (Figure 4bI and II). Neither $\text{PGF}_{2\alpha}$ nor bimatoprost activated the altFP4 receptor (Figure 4cI and II). To

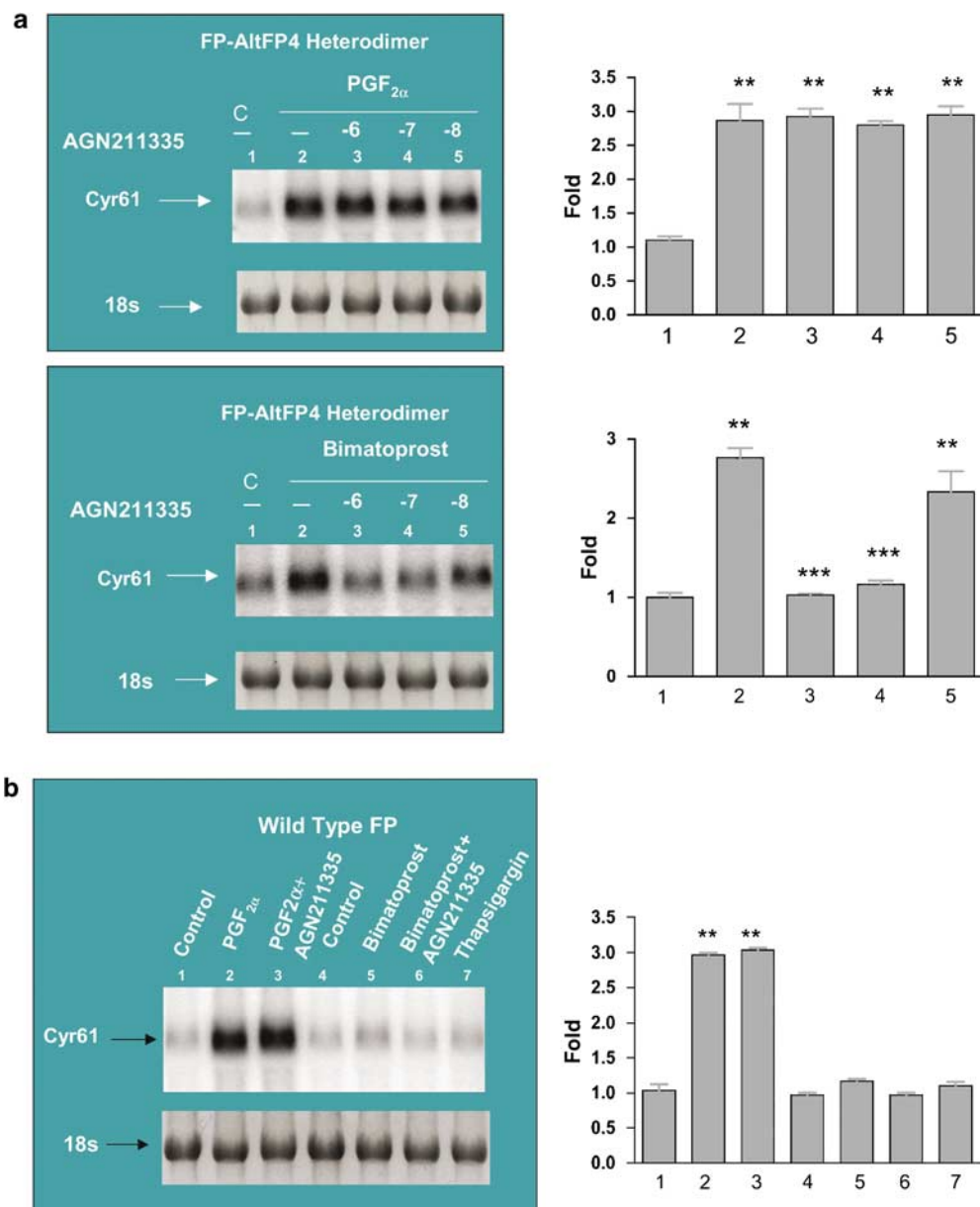


Figure 6 Northern blot analysis of Cyr61 gene expression following prostaglandin F_{2α} (PGF_{2α}) and bimatoprost treatment. (a) HEK293/EBNA cells co-expressing FP and altFP4 receptors were pretreated with 10⁻⁶–10⁻⁸ M AGN211335 for 15 min (a, top and bottom panels, lanes 3–5) and with 10⁻⁷ M PGF_{2α} for 1 h (a, top panel, lanes 2–5) or with 10⁻⁷ M bimatoprost for 1 h (a, bottom panel, lanes 2–5). Arrows indicate Cyr61 mRNA levels. (a, right panels) The data represent mean ± s.d. of three independent densitometric experiments. ***P* < 0.01 versus control; ****P* < 0.01 versus bimatoprost alone. The intensities of the 18S rRNA bands were used to normalize the RNA-loading differences. (b) HEK293/EBNA cells expressing FP receptor were pretreated with 10⁻⁶ M AGN211335 for 15 min (lanes 3 and 6) and with 10⁻⁷ M PGF_{2α} for 1 h (lanes 2 and 3) or with 10⁻⁷ M bimatoprost for 1 h (lanes 5 and 6) or with 2 μM thapsigargin for 15 min (lane 7). Arrows indicate Cyr61 mRNA levels. (b, right panel) The data represent mean ± s.d. of three independent densitometric experiments. ***P* < 0.01 versus control. The intensities of the 18S rRNA bands were used to normalize the RNA-loading differences.

investigate further the mechanism of the second-phase Ca²⁺ signal initiated by bimatoprost, Ca²⁺-free buffer was used in the FLIPR assay. Both PGF_{2α} and bimatoprost elicited a rapid increase in intracellular Ca²⁺ concentration followed by an immediate return to baseline (Figure 4dI and II), suggesting that the bimatoprost-initiated second-phase Ca²⁺ mobilization may be attributed to store-operated Ca²⁺ influx. The data are summarized in Figure 4e. To determine whether the bimatoprost-initiated second-phase Ca²⁺ mobilization is

due to Ca²⁺ release from a second intracellular Ca²⁺ store, thapsigargin, a Ca²⁺-ATPase inhibitor, was used to deplete the endoplasmic reticulum Ca²⁺ store in the cells before bimatoprost treatment. The experiments showed that there is no further Ca²⁺ release upon bimatoprost treatment after endoplasmic reticulum Ca²⁺ stores were completely depleted, suggesting that bimatoprost-initiated second-phase Ca²⁺ mobilization may not be due to the release of Ca²⁺ from a second intracellular Ca²⁺ store (data not shown).

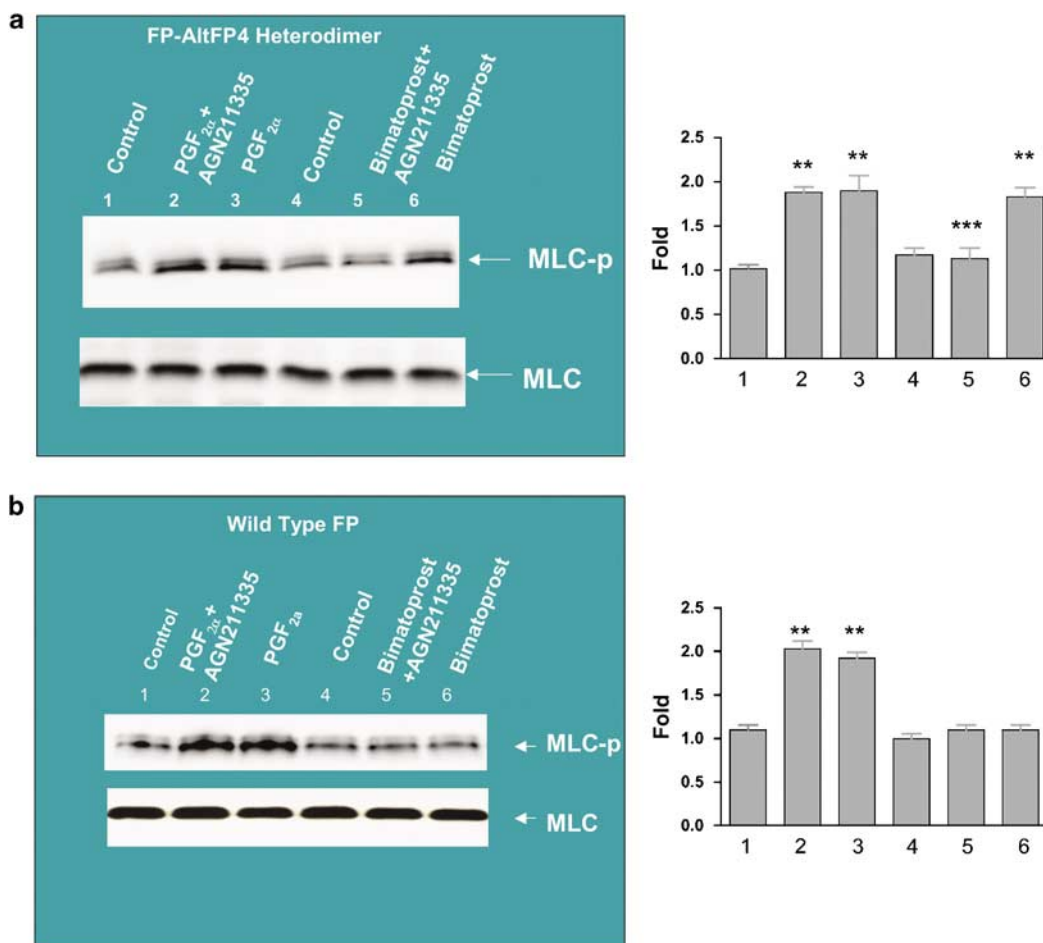


Figure 7 Effects of prostaglandin F_{2α} (PGF_{2α}) and bimatoprost on myosin light chain (MLC) phosphorylation. (a) HEK293/EBNA cells co-expressing FP and altFP4 receptors were pretreated with 10⁻⁶ M AGN211335 for 15 min (lanes 2 and 5) and with 10⁻⁷ M PGF_{2α} for 30 min (lanes 2 and 3) or with 10⁻⁷ M bimatoprost for 30 min (lanes 5 and 6). Arrows indicate MLC phosphorylation. (a, right panel) The data represent mean ± s.d. of three independent experiments. ***P* < 0.01 versus control; ****P* < 0.01 versus bimatoprost alone. The intensities of the total MLC bands were used to normalize the protein-loading differences. (b) HEK293/EBNA cells expressing the FP receptor were pretreated with 10⁻⁶ M AGN211335 for 15 min (lanes 2 and 5) and with 10⁻⁷ M PGF_{2α} for 30 min (lanes 2 and 3) or with 10⁻⁷ M bimatoprost for 30 min (lanes 5 and 6). Arrows indicate MLC phosphorylation. (b, right panel) The data represent mean ± s.d. of three independent experiments. ***P* < 0.01 versus control. The intensities of the total MLC bands were used to normalize the protein-loading differences.

More importantly, the prostamide antagonist, AGN211335, selectively inhibited the bimatoprost-initiated second phase of Ca²⁺ mobilization in HEK293/EBNA cells co-expressing FP and altFP4 receptors, in a dose-dependent manner (Figure 5bI–IV), but did not block the steady-state phase of that induced by PGF_{2α} (Figure 5aI–IV). A summary of these data is shown in Figure 5c and d.

To determine whether the prostamide antagonist selectively blocks bimatoprost-induced biochemical signal cascades, we used the Cyr61 factor and MLC as biochemical signals to perform Cyr61 mRNA expression studies and MLC phosphorylation studies. Cyr61 has been well-characterized and regulates extracellular matrix remodelling through activation of matrix metalloproteinases (Liang *et al.*, 2003). Phosphorylation of MLC causes ciliary muscle contraction with a resultant widening of intermuscular spaces (Ansari *et al.*, 2003). Increases in uveoscleral outflow result from extracellular matrix remodelling of the ciliary body and widened intermuscular spaces. Both PGF_{2α} and bimatoprost

induced Cyr61 mRNA upregulation and MLC phosphorylation in HEK293/EBNA cells co-expressing FP and altFP4 receptors (Figures 6a and 7a). Even though PGF_{2α} induced Cyr61 mRNA upregulation and MLC phosphorylation in HEK293/EBNA cells expressing the wild-type FP receptor, bimatoprost produced no effects (Figure 6b). The prostamide antagonist, AGN211335, selectively blocked both bimatoprost-induced Cyr61 mRNA upregulation and bimatoprost-induced MLC phosphorylation in HEK293/EBNA cells co-expressing FP and altFP4 receptors, but not those induced by PGF_{2α} (Figures 6a and 7a). We also investigated the effects of thapsigargin, as it activates store-operated channels independently of G protein-coupled receptors. However, it failed to induce Cyr61 mRNA upregulation (Figure 6b), indicating that induction of Cyr61 mRNA upregulation requires more signal transduction pathways, possibly those involving the activation of G_{12/13} and RhoA (Liang *et al.*, 2003). These data fit well with the prostamide antagonist profile, which selectively inhibits bimatoprost-induced feline iris contraction, but not that produced by PGF_{2α}.

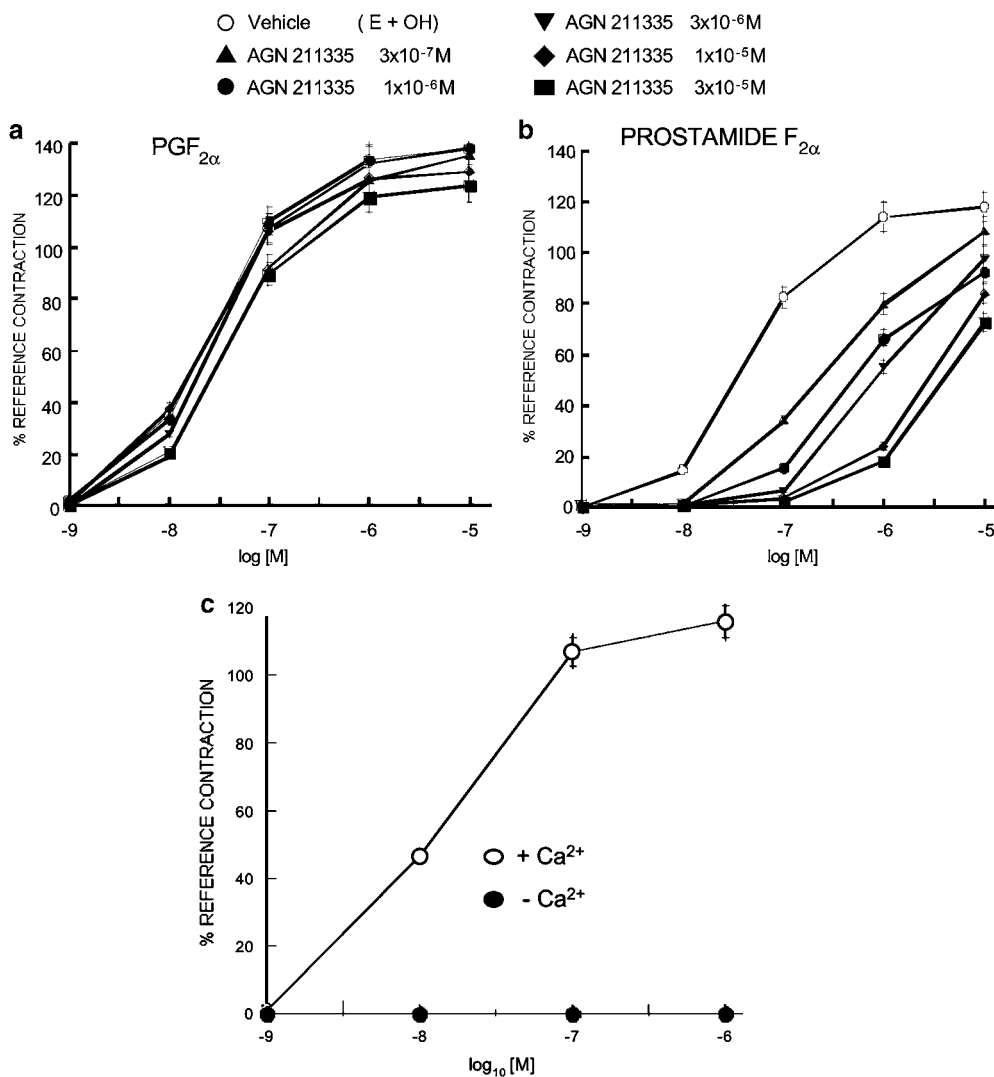


Figure 8 Effect of graded doses of AGN211335 on contractions of the feline isolated iris. (a) Effect of AGN211335, 3×10^{-7} – 3×10^{-5} M, compared to vehicle on responses produced by prostaglandin F_{2α} (PGF_{2α}). (b) Effect of the same concentrations of AGN211335, compared to vehicle, on responses produced by prostamide F_{2α}. (c) Effect of bimatoprost, in the absence and presence of Ca²⁺ in the physiological buffer, on the isolated iris. Values are mean ± s.e.mean, *n* = 4.

Pharmacological characterization of the prostamide antagonist AGN211335. The effects of graded doses of AGN211335 pretreatment on feline iridial contraction produced by PGF_{2α} and prostamide F_{2α} are depicted in Figure 8. AGN211335, over the dose range 3×10^{-7} – 3×10^{-5} M, did not have a significant effect on the iridial response to PGF_{2α} (Figure 8a). In marked contrast, and at all the doses used, AGN211335 produced a dose-dependent rightward shift of the prostamide dose–response curve (Figure 8b). Thus, in a single preparation, AGN211335 selectively blocks the prostamide effect without altering the response to PGF_{2α}. As described in a previous study (Woodward *et al.*, 2007), the antagonist effects were never totally surmounted by 10 μM prostamide F_{2α}; this has been attributed to off-target activity for prostamide F_{2α} at prostanoid FP receptor in the feline iris (Matias *et al.*, 2004; Spada *et al.*, 2005). The AGN211335 antagonism of the prostamide F_{2α} was subjected to Schild analysis, as previously described (Woodward *et al.*, 2007). AGN211335 appeared to be a competitive antagonist with a

pA₂ of 7.50. Finally, bimatoprost stimulation of feline iridial contraction did not occur in Ca²⁺-free medium (Figure 8c).

AGN211335 was screened for activity at other prostaglandin receptors using the full range of human recombinant receptors. No activity was observed at DP_{1–2}, EP_{1–4}, FP or IP receptors for 3×10^{-5} M AGN211335. AGN211335 is also a TP antagonist, with a *K_b* of 101 nM, but is less potent as a TP receptor antagonist than the prototype prostamide antagonist AGN204396 (Woodward *et al.*, 2007). As functional TP receptors are not present in the feline iris preparation, this activity of AGN211335 does not interfere with the analysis of FP and prostamide receptor pharmacology.

Discussion

The pharmacology and physiological significance of truncated prostanoid receptors lacking an intracellular carboxyl terminus has remained obscure. Although transcripts for

such truncated isoforms of FP (Vielhauer *et al.*, 2004) and EP₁ (Okuda-Ashitaka *et al.*, 1996) receptors were found in tissues, no ligand-dependent activation was observed (Okuda-Ashitaka *et al.*, 1996; Vielhauer *et al.*, 2004). Likewise, the FP receptor variants described herein show no meaningful G protein-coupled receptor-like activity. However, these novel FP receptor mRNA splicing variants are capable of heterodimerization with wild-type FP receptors. These heterodimers are distinct from the component monomers in terms of both ligand recognition and Ca²⁺ signalling. For PGF_{2α}, wild-type FP and the FP-altFP4 heterodimer respond in an identical manner with a Ca²⁺ transient followed by an elevated steady-state phase. These heterodimers differ from wild-type FP receptors in that they appear highly responsive to the prostamide analogue bimatoprost (Woodward *et al.*, 2003; Matias *et al.*, 2004). Moreover, interaction with bimatoprost results in a biphasic Ca²⁺ signal composed of a rapid transient response succeeded by secondary Ca²⁺ waves. The transient phase represents Ca²⁺ release from intracellular stores. The secondary phase appears to involve Ca²⁺ influx and is absent when extracellular Ca²⁺ is removed. The secondary phase of Ca²⁺ signalling is susceptible to the prostamide antagonist AGN211335. This suggests that FP-altFP receptor heterodimerization may represent the putative prostamide receptor (Gandolfi and Cimino, 2003; Woodward *et al.*, 2003, 2007; Matias *et al.*, 2004).

There are a number of close correlations between the FP-altFP recombinant receptor model and prostamide pharmacology observed in cells, tissues and living animals. To date, prostamide F_{2α} and bimatoprost have been found to be active only in cells and tissues that express functional prostanoid FP receptors (Woodward *et al.*, 2001, 2003, 2007; Liang *et al.*, 2003; Richter *et al.*, 2003; Matias *et al.*, 2004). This is consistent with the presence of FP-altFP heterodimers, which are responsive to prostamides and are indistinguishable from FP receptors with respect to PGF_{2α} effects. A close connection to the FP receptor gene is further indicated by studies claiming that the ocular hypotensive effect of bimatoprost is absent in *-/-*FP mice (Crowston *et al.*, 2005; Ota *et al.*, 2005). Upregulation of Cyr61 appears to be a common upstream event in the initiation of ciliary muscle re-modelling and resultant increases in uveoscleral outflow, which are common to ocular hypotensive prostamides, FP and EP₂ receptor agonists (Liang *et al.*, 2003; Richter *et al.*, 2003). As human ciliary muscle cells are sensitive to bimatoprost, mRNA for the newly discovered altFP variants would be expected to be present in these cells, and this has been shown to be the case.

The discovery of selective antagonists has been of paramount importance in defining prostamide pharmacology. The prototypical prostamide antagonist AGN204396 was described in 2007 (Woodward *et al.*, 2007), but since then, rapid progress has occurred. Second-generation prostamide antagonists, such as AGN211334, which has been shown to block bimatoprost activity in human eye perfusion model (Wan *et al.*, 2007) and AGN211335, are approximately 100 times more potent than their prototype. The susceptibility of the bimatoprost-induced secondary Ca²⁺ influx response in FP-altFP heterodimer to blockade by AGN211335 applies to all prostamide-sensitive preparations. The lack of inhibition

afforded by AGN211335 on PGF_{2α}-induced Ca²⁺ signalling in the FP-altFP receptor model similarly applies to prostamide-sensitive cells and tissues. Thus, AGN211335 dose-dependently blocks the feline iridial response to prostamide F_{2α} but not to PGF_{2α}. It is important to note that feline iridial contraction is entirely dependent on extracellular Ca²⁺. It follows that AGN211335 inhibition of the prostamide-induced secondary Ca²⁺ signals associated with FP-altFP heterodimer also correlates with Ca²⁺-dependent contraction of feline iridial tissue. To date, there is no feline FP gene structure available in a public database. It is not known if altFPs are expressed in feline iridial tissue. As it is established that the effects of prostamides and the prostamide antagonist AGN211335 in the FP-altFP4 receptor model correspond closely to those in the feline iridial contractile response model, it is reasonable for us to speculate that feline iridial tissue may express FP-altFP heterodimers that are sensitive to prostamide F_{2α} and AGN211335. The mechanism of the AGN211335-insensitive transient release of intracellular Ca²⁺ produced by bimatoprost is not readily apparent. It appears that the FP-altFP4 heterodimer maintains responsiveness to PGF_{2α} and acquires sensitivity to prostamides, with a common initial Ca²⁺ signalling pathway, involving release of Ca²⁺ from intracellular stores. Thereafter, the Ca²⁺ signalling pathways diverge, as reflected by subsequent phases that are pharmacologically and qualitatively distinct. Antagonism of recombinant and native prostamide-sensitive FP-altFP heterodimeric receptors extends beyond Ca²⁺ signalling and smooth muscle contraction. Bimatoprost-induced Cyr61 mRNA upregulation in human ciliary smooth muscle cells is replicated in the FP-altFP4 heterodimeric receptor model and, importantly, is blocked by the prostamide antagonist AGN211335 (Liang *et al.*, 2003). Finally, bimatoprost-induced MLC phosphorylation associated with FP-altFP4 heterodimeric receptors was blocked by AGN211335. Again, in the case of both MLC phosphorylation and Cyr61 upregulation, PGF_{2α} effects were not affected by pretreatment with the prostamide antagonist AGN211335.

The action of prostamides has been found to involve mechanisms different from prostanoid FP receptor-mediated responses in the primate eye. First, the effect of bimatoprost in the ocular hypertensive monkey model of glaucoma (Gagliuso *et al.*, 2004) has been shown to be additive to that of latanoprost, the FP receptor agonist prodrug (Resul *et al.*, 1997). This fits with the FP-altFP heterodimeric receptor concept, as divergent secondary Ca²⁺ signalling pathways may translate into an additive effect for prostamides and prostanoid FP receptor agonists on IOP. A pharmacological distinction between bimatoprost and latanoprost has also been made at the clinical level. Glaucomatous human subjects refractory to latanoprost treatment were found to be susceptible to bimatoprost, which produced a marked reduction of IOP (Gandolfi and Cimino, 2003). This fits particularly well with the FP-altFP heterodimer prostamide receptor hypothesis as both bimatoprost and latanoprost would be expected to be active. The recent discovery that certain single-nucleotide polymorphisms associated with the FP receptor account for latanoprost insensitivity in the human eye (Sakurai *et al.*, 2007) may be explained by

the following hypothesis: heterodimerization of the mutated wt FP receptor with an alternative mRNA splicing variant of the FP receptor becomes insensitive to anionic FP receptor agonists but retains sensitivity to bimatoprost.

It is now well-established that receptors of the G protein-coupled receptor variety form heterodimers and that these can dramatically alter receptor function in terms of ligand recognition, second messenger signalling and receptor trafficking (Jordan and Devi, 1999; Breitweiser, 2004; Wilson *et al.*, 2004; Bulenger *et al.*, 2005; Prinster *et al.*, 2005). Heterodimerization may create an entirely unique receptor-binding site (Jordan and Devi, 1999; Wilson *et al.*, 2004). Prostanoid receptors have also been shown to dimerize; these occur as an EP_{1/α2}-adrenoceptor heterodimeric complex (McGraw *et al.*, 2006) and dimerization of the IP receptor and the TP_α receptor isoform (Wilson *et al.*, 2004). In terms of second messenger signalling, the IP/TP_α heterodimer confers PGI₂-like properties to thromboxane mimetics in the form of robust TP receptor-mediated cAMP generation (Wilson *et al.*, 2004). An alternative binding site for isoprostane E₂ was apparently created in the case of IP/TP_α, which may be regarded as analogous to the prostamide recognition site apparent for the FP-altFP heterodimer. Isoprostane E₂-induced increases in cAMP have been shown to be dependent on TP receptor expression, but are not inhibited by the TP antagonist SQ 29548, which sets them apart from the IP/TP_α heterodimer (Wilson *et al.*, 2004). Formation of a further ligand-binding site is a frequent occurrence of G protein-coupled receptor dimerization (Jordan and Devi, 1999; Breitweiser, 2004; Prinster *et al.*, 2005), and prostanoid receptor heterodimeric complexes appear to be no exception. For IP/TP_α, a unique isoprostane E₂ binding site occurs. In the case of FP-altFP, prostamide responsiveness is conferred.

Prostaglandin receptor heterodimerization within and outside the prostanoid receptor classification has already been shown to have important physiological implications (Jordan and Devi, 1999; Breitweiser, 2004; Wilson *et al.*, 2004; Bulenger *et al.*, 2005; Prinster *et al.*, 2005; McGraw *et al.*, 2006). EP_{1/α2}-adrenoceptor heterodimerization has an impact on airway tone, in that EP₁ receptor stimulation may reduce α₂-adrenoceptor-mediated cAMP formation and resultant bronchodilatation (McGraw *et al.*, 2006). The IP/TP_α heterodimer may influence the thromboxane/prostacyclin balance by providing an additional PGI₂-like effect to oppose and limit TP_α-mediated effects (Wilson *et al.*, 2004). Novel ligand-recognition sites emerge as a result of prostanoid-prostanoid receptor heterodimerization. Thus, an isoprostane binding site is created by the IP/TP_α heterodimers (Wilson *et al.*, 2004). The FP-altFP receptor heterodimers confer prostamide sensitivity, which is lacking in wild-type FP receptors. It is not easy to rule out the possibility that the FP-altFP heterodimers are putative prostamide receptors. It appears that prostamide activity observed in freshly isolated cells (Gagliuso *et al.*, 2004; Spada *et al.*, 2005) and tissues (Woodward *et al.*, 2003, 2007; Matias *et al.*, 2004), such as the feline iris described here, may be modelled by a recombinant system involving co-expression of FP and altFP receptors, as suggested by the effects of bimatoprost.

Conflict of interest

The authors state no conflict of interest.

References

- Adams JW, Migita DS, Yu MK, Young R, Hellickson MS, Castro-Vargus FE *et al.* (1996). Prostaglandin F₂ alpha stimulates hypertrophic growth of cultured neonatal rat ventricular myocytes. *J Biol Chem* **271**: 1179–1186.
- Ansari HR, Davis AM, Kaddour-Djebbar I, Abdel-Latif AA (2003). Effects of prostaglandin F₂alpha and latanoprost on phosphoinositide turnover, myosin light chain phosphorylation and contraction in cat iris sphincter. *J Ocul Pharmacol Ther* **19**: 217–231.
- Arunlakshana O, Schild HO (1959). Some quantitative use of drug antagonists. *Br J Pharmacol Chemother* **257**: 48–58.
- Berglund BA, Boring DL, Howlett AC (1999). Investigation of structural analogs of prostaglandin amides for binding to and activation of CB and CB₂ cannabinoid receptors in rat brain and human tonsils. *Adv Exp Med Biol* **469**: 527–533.
- Breitweiser GA (2004). G protein-coupled receptor oligomerization: implications for G protein activation and cell signaling. *Circ Res* **94**: 17–27.
- Bulenger S, Marullo S, Bouvier M (2005). Emerging role of homo- and heterodimerization in G-protein-coupled receptor biosynthesis and maturation. *Trends Pharmacol Sci* **26**: 131–137.
- Burstein SH, Rossetti RG, Yagen B, Zurier RB (2000). Oxidative metabolism of anandamide. *Prostaglandins Other Lipid Mediat* **61**: 29–41.
- Crowston JG, Lindsey JD, Morris CA, Wheeler L, Medeiros FA, Weinreb RN (2005). Effect of bimatoprost on intraocular pressure in prostaglandin FP receptor knockout mice. *Invest Ophthalmol Vis Sci* **46**: 4571–4577.
- Fujino H, Srinivasan D, Pierce KL, Regan JW (2000). Differential regulation of prostaglandin F₂(alpha) receptor isoforms by protein kinase C. *Mol Pharmacol* **57**: 353–358.
- Gagliuso DJ, Wang RF, Mittag TW, Podos SM (2004). Additivity of bimatoprost or travoprost to latanoprost in glaucomatous monkey eyes. *Arch Ophthalmol* **122**: 1342–1347.
- Gandolfi SA, Cimino L (2003). Effect of bimatoprost on patients with primary open-angle glaucoma or ocular hypertension who are nonresponders to latanoprost. *Ophthalmol* **110**: 609–614.
- Gaton DD, Sagart T, Lindsey JD, Gabelt BAT, Kaufman PL, Weinreb RN (2001). Increased matrix metalloproteinases 1, 2, and 3 in the monkey uveoscleral outflow pathway after topical prostaglandin F₂(alpha)-isopropyl ester treatment. *Arch Ophthalmol* **119**: 1165–1170.
- Horton EW, Poyser NL (1976). Uterine luteolytic hormone: a physiological role for prostaglandin F₂alpha. *Physiol Rev* **56**: 595–651.
- Jordan BA, Devi LA (1999). G-protein-coupled receptor heterodimerization modulates receptor function. *Nature* **399**: 697–700.
- Koda N, Tsutsui Y, Niwa H, Ito S, Woodward DF, Waternabe K (2003). Synthesis of prostaglandin F ethanamide by prostaglandin F synthase and identification of bimatoprost as a potent inhibitor of the enzyme: new enzyme method by LC/GSI/MS. *Arch Biochem Biophys* **424**: 128–136.
- Kolodziej PA, Young RA (1991). Epitope tagging and protein surveillance. *Methods Enzymol* **194**: 508–519.
- Kozak KR, Crews BC, Ray JL, Tai HH, Morrow JD, Marnett LJ (2001). Metabolism of prostaglandin glyceryl esters and prostaglandin ethanalamides *in vitro* and *in vivo*. *J Biol Chem* **276**: 36993–36998.
- Liang Y, Li C, Guzman VM, Evinger III AJ, Protzman CE, Krauss A-H *et al.* (2003). Comparison of prostaglandin F₂alpha, bimatoprost (prostamide), and butaprost (EP₂ agonist) on Cyr61 and connective tissue growth factor gene expression. *J Biol Chem* **278**: 27267–27277.
- Matias I, Chen J, Petrocellis LD, Bisognot T, Ligresti A, Fezza F *et al.* (2004). Prostaglandin ethanalamides (prostamides): *in vitro* pharmacology and metabolism. *J Pharmacol Exp Ther* **309**: 745–757.
- McGraw DW, Mihlbachler KA, Schwarb MR, Rahman FR, Small KM, Almoosa KF *et al.* (2006). Airway smooth muscle prostaglandin-

- EP1 receptors directly modulate beta2-adrenergic receptors within a unique heterodimeric complex. *J Clin Invest* **116**: 1400–1409.
- Okuda-Ashitaka E, Sakamoto K, Ezashi KM, Ito S, Hayaishi O (1996). Suppression of prostaglandin E receptor signaling by the variant form of EP1 subtype. *J Biol Chem* **271**: 31255–31261.
- Ota T, Aihara M, Narumiya S, Araie M (2005). The effects of prostaglandin analogues on IOP in prostanoid FP-receptor-deficient mice. *Invest Ophthalmol Vis Sci* **46**: 4159–4163.
- Prinster SC, Hauge C, Hall RA (2005). Heterodimerization of G protein-coupled receptors: specificity and functional significance. *Pharmacol Rev* **57**: 289–298.
- Resul B, Stjerschantz J, Selen G, Bito L (1997). Structure–activity relationships and receptor profiles of some ocular hypotensive prostanoids. *Surv Ophthalmol* **41**: 47–52.
- Richter M, Krauss AH, Woodward DF, Lutjen-Drecoll E (2003). Morphological changes in the anterior eye segment after long-term treatment with different receptor selective prostaglandin agonists and a prostamide. *Invest Ophthalmol Vis Sci* **44**: 4419–4426.
- Ross RA, Craib SJ, Stevenson LA, Pertwee RG, Henderson A, Toole J *et al.* (2002). Pharmacological characterization of the anandamide cyclooxygenase metabolite: prostaglandin E2 ethanolamide. *J Pharmacol Exp Ther* **301**: 900–907.
- Sakurai M, Higashide T, Takahashi M, Sugiyama K (2007). Association between genetic polymorphisms of the prostaglandin F2alpha receptor gene and response to latanoprost. *Ophthalmol* **114**: 1039–1046.
- Smith WL, Marnett LJ, Dewitt DL (1991). Prostaglandin and thromboxane biosynthesis. *Pharmacol Ther* **49**: 153–179.
- Spada CS, Krauss AH, Woodward DF, Chen J, Protzman CE, Nieves AL *et al.* (2005). Bimatoprost and prostaglandin F(2 alpha) selectively stimulate intracellular calcium signaling in different cat iris sphincter cells. *Exp Eye Res* **80**: 135–145.
- Toh H, Ichikawa A, Narumiya S (1995). Molecular evolution of receptors for eicosanoids. *FEBS Lett* **361**: 17–21.
- Vielhauer GA, Fujino H, Regan JW (2004). Cloning and localization of hFP(S): a six-transmembrane mRNA splice variant of the human FP prostanoid receptor. *Arch Biochem Biophys* **421**: 175–185.
- Wan Z, Woodward DF, Cornell C, Fliri H, Martos J, Pettit S *et al.* (2007). Bimatoprost, prostamide activity, and conventional drainage. *Invest Ophthalmol Vis Sci* **48**: 4107–4115.
- Weinreb RN, Lindsey JD (2002). Metalloproteinase gene transcription in human ciliary muscle cells with latanoprost. *Invest Ophthalmol Vis Sci* **43**: 716–722.
- Wilson SJ, Roche AM, Kostetskaia E, Smyth EM (2004). Dimerization of the human receptors for prostacyclin and thromboxane facilitates thromboxane receptor-mediated cAMP generation. *J Biol Chem* **279**: 53036–53047.
- Woodward DF, Krauss AH, Chen J, Lai RK, Spada CS, Burk RM *et al.* (2001). The pharmacology of bimatoprost (Lumigan). *Surv Ophthalmol* **45**: S337–S345.
- Woodward DF, Krauss AHP, Chen J, Liang Y, Li C, Protzman E *et al.* (2003). Pharmacological characterization of a novel antiglaucoma agent, Bimatoprost (AGN 192024). *J Pharmacol Exp Ther* **305**: 772–785.
- Woodward DF, Krauss AHP, Wang JW, Protzman CE, Nieves AL, Liang Y *et al.* (2007). Identification of an antagonist that selectively blocks the activity of prostamides (prostaglandin- ethanolamides) in the feline iris. *Br J Pharmacol* **150**: 342–352.
- Woodward DF, Lawrence RA, Fairbairn CE, Shan T, Williams LS (1993). Intraocular pressure effects of selective prostanoid receptor agonists involve different receptor subtypes according to radioligand binding studies. *J Lipid Mediat* **6**: 545–553.
- Yu M, Ives D, Ramesh CS (1997). Synthesis of prostaglandin E2 ethanolamide from anandamide by cyclooxygenase-2. *J Biol Chem* **272**: 21181–21186.

BJP Open This article is available free of charge on the BJP website (<http://www.brjpharmacol.org>).